VERSITA

INTERNATIONAL
Agrophysics
www.international-agrophysics.org

Int. Agrophys., 2013, 27, 31-37
doi: 10.2478/v10247-012-0065-z

Prediction of long-term groundwater recharge by using hydropedotransfer functions

K. Miegel[1], *K. Bohne*[1]*, *and G. Wessolek*[2]

[1]Faculty of Agricultural and Environmental Sciences, University of Rostock, Satower 48, 18051 Rostock, Germany
[2]Department of Ecology, Technical University Berlin, School IV, Ernst-Reuter-Platz 1, 10587 Berlin, Germany

Received July 4, 2012; accepted September 3, 2012

A b s t r a c t. The investigations to estimate groundwater recharge were performed. Improved consideration of soil hydrologic processes yielded a convenient method to predict actual evapotranspiration and hence, groundwater recharge from easily available data. For that purpose a comprehensive data base was needed, which was created by the simulation model SWAP comprising 135 different site conditions and 30 simulation years each. Based upon simulated values of actual evapotranspiration, a transfer function was developed employing the parameter b in the Bagrov differential equation $dE_a/dP = 1 - (E_a/E_p)^b$. Under humid conditions, the Bagrov method predicted long-term averages of actual evapotranspiration and groundwater recharge with a standard error of 15 mm year^{-1} (R = 0.96). Under dry climatic conditions and groundwater influence, simulated actual evapotranspiration may exceed precipitation. Since the Bagrov equation is not valid under conditions like these, a statistic-based transfer function was developed predicting groundwater recharge including groundwater depletion with a standard error of 26 mm (R = 0.975). The software necessary to perform calculations is provided online.

K e y w o r d s: evapotranspiration, groundwater, simulation, capillary rise

INTRODUCTION

Long-term total runoff (R) is one of the most desired hydrological information. Measured data of R often are not available. Especially in ungauged catchments mathematical methods are necessary to calculate R. In such cases R is accessible as:

$$R = P - E_a, \tag{1}$$

where: P is the annual amount of rain corrected for systematic observation errors and E_a is the actual evapotranspiration. If surface runoff and interflow are negligible, R may be seen as groundwater recharge. Provided that these preconditions are fulfilled, the estimation of E_a is the central issue to solve Eq. (1). Application of a comprehensive soil water simulation model would yield the desired results but such a model requires a lot of input data, which are often not available. To facilitate matters, hydropedotransfer functions (HPTF) have been developed, which relate easily available site information and meteorological data to required results. Recently, Wessolek *et al*. (2008, 2011) have shown that HPTF are valuable tools to predict annual percolation rates on a regional scale. Unfortunately, it is risky to use stochastic methods outside the range of conditions where they were developed. With regard to broader applicability, physically based methods are more promising.

The approach described here employs the method of Bagrov which was successfully used by Bonta and Müller (1999), Glugla and Tiemer (1971), Glugla *et al*. (2003), among others. This method is combined with a new transfer function to evaluate the effect of site conditions on actual evapotranspitration.

MATERIAL AND METHODS

To create a surrogate reality providing the data basis needed, we used the well documented numerical simulation program SWAP (Kroes and van Dam, 2003; Kroes *et al*., 1999). Based on a numerical solution of the Richards equation, this model simulates transient transport of water, heat and solutes in soils due to changing boundary conditions. The SWAP program incorporates many years of research and was extensively tested by several research groups. Details of these investigations are reported by van Dam *et al.* (2008). The model describes soil hydraulic properties by the Mualem-van Genuchten equations (van Genuchten, 1980), whose parametes were taken from a data base (Renger *et al*., 2009) that provides characteristic data of soil texture classes (Table 1). From these, 14 soils were selected for simulation

*Corresponding author e-mail: klaus.bohne@uni-rostock.de

T a b l e 1. Soil hydraulic parameters of the Mualem-van Genuchten model (van Genuchten, 1980) for soil classes corresponding to German soil texture classes

Texture class	Clay (%)	Silt (%)	θ_r (cm^3 cm^{-3})	θ_s (cm^3 cm^{-3})	α hPa^{-1}	n 1	x 1	K_0 (cm day^{-1})
Ss	0-5	0-10	0	0.3879	0.2644	1.3515	-0.59	512
Sl2	5-7	5-20	0	0.3949	0.1165	1.2542	0	192
Sl3	7-12	5-40	0.0519	0.3952	0.07097	1.3510	0	90
Sl4	13-17	13-40	0	0.4101	0.1049	1.1843	-3.24	141
Slu	7-15	40-50	0	0.4138	0.08165	1.177	-3.92	109
St2	5-15	0-10	0	0.4049	0.4846	1.1883	-6.19	420
St3	15-25	0-13	0	0.4214	0.1802	1.1323	-3.42	306
Su2	0-5	10-25	0	0.3786	0.2039	1.2347	-3.34	285
Su3	0-7	25-40	0	0.3764	0.08862	1.2140	-3.61	120
Su4	0-7	40-50	0	0.3839	0.3839	1.2223	-3.74	83
Ls2	15-25	40-50	0.1406	0.4148	0.04052	1.3242	-2.07	38
Ls3	15-25	27-40	0.0336	0.4092	0.06835	1.2050	-3.23	98
Ls4	17-20	15-25	0.0463	0.4129	0.09955	1.1821	-3.6	170
Lt2	25-35	35-50	0.1490	0.4380	0.07013	1.2457	-3.18	62
Lt3	35-45	30-50	0.1629	0.4530	0.04947	1.1700	-4.10	44
Lts	25-45	17-35	0.1154	0.4325	0.03401	1.1944	0	52
Lu	17-28	50-70	0.0534	0.4284	0.04321	1.1652	-3.23	83
Uu	0-7	80-100	0	0.4030	0.01420	1.2134	-0.56	34
Uls	7-13	50-65	0	0.3985	0.02260	1.1977	-2.04	40
Us	0-7	50-80	0	0.3946	0.02747	1.2239	-2.73	35
Ut2	7-13	>50	0.01011	0.4001	0.01868	1.2207	-1.38	29
Ut3	13-17	>50	0.00532	0.4030	0.01679	1.2067	-1.20	28
Ut4	17-24	>50	0.02764	0.4162	0.01697	1.2048	-0.77	25
Tt	67-100	0-30	0	0.5238	0.06612	1.0522	0	155
Tl	47-67	17-30	0	0.4931	0.07339	1.0625	0	172
Tu2	47-67	>30	0	0.4971	0.07242	1.0606	0	179
Tu3	37-47	>40	0	0.4589	0.0550	1.0817	0	124
Tu4	25-35	>45	0.0170	0.4372	0.04538	1.1204	0	89
Ts2	51-67	0-17	0	0.4836	0.08402	1.0767	0	250
Ts3	35-51	0-17	0.07841	0.4374	0.06194	1.1456	0	118
Ts4	25-35	0-17	0	0.4355	0.2092	1.1142	-7.61	322
fS	0-5	0-10	0	0.4095	0.1504	1.3358	-0.33	285
mS	0-5	0-10	0	0.3886	0.2619	1.3533	-0.58	507
gS	0-5	0-10	0	0.3768	0.2206	1.4657	1.38	872

K_0 is a parameter chosen to fit data of unsaturated soil hydraulic conductivity, parameter x denotes the tortuosity parameter, the van Genuchten model is given by $\theta = \theta_r + (\theta_s - \theta_r) / (1 + (\alpha h)^n)^{(1-1/n)}$.

T a b l e 2. Selected soil classes with assumed soil properties

Class of		Root depth (cm)	FC	PWP	HLIM evapotranspiration (cm)	
soil hydraulic*	texture		(cm^3 cm^{-3})		high	low
A1	Ss	60	0.143	0.021	-212	-500
A2	Sl2	60	0.234	0.058	-271	-705
A3	Su3	60	0.255	0.080	-307	-827
A4	Ls3	90	0.331	0.174	-253	-616
B1	Uu	90	0.361	0.127	-443	-1156
B2	Uls	90	0.340	0.126	-393	-1059
B3	Slu	90	0.303	0.116	-344	-955
B3	Ls2	90	0.331	0.174	-253	-616
B3	Lt2	90	0.344	0.20	-287	-751
C1	Tt	90	0.481	0.364	-529	-1551
C2	Ts2	90	0.421	0.278	-475	-1391
C2	Ts3	90	0.366	0.210	-389	-1101
C3	Tu2	90	0.442	0.320	-510	-1495
C4	Lts	90	0.374	0.209	-367	-993

*Twarakavi *et al*. (2010). FC – water content at h_p = -63 cm (field capacity), PWP – water content at h_p = -15 800 cm (permanent wilting point), HLIM denotes the soil water pressure head from where E_a/E_p decreases linearly from unity to zero, which is given at the permanent wilting point.

(Table 2). The range of soils selected for this investigation covers the hydraulic soil classes proposed by Twarakavi (2010). To consider hysteresis, the parameter α was doubled (Luckner *et al*., 1989). Effects of macroporosity and preferential flow were not taken into account.

In this study, the soil profile was subdivided into compartments of 1 cm thickness near the soil surface increasing downward up to 20 cm. The total simulation depth was 300 cm. To establish initial conditions, the soil profiles were assumed to be in hydrostatic equilibrium with the groundwater table (Jury *et al*., 1991). Since equilibration takes a very long time in the dry range, the soil pressure head was restricted to be > - 63 hPa. The top of the soil profile was ruled by atmospheric boundary conditions as provided by the SWAP model. To establish bottom boundary conditions, two options were used. In the case of soil profiles without groundwater influence, free drainage under a unit hydraulic gradient was assumed. Groundwater affected soils were simulated by a pressure head boundary condition. For each of the soil classes considered, simulation runs were performed using values of the groundwater table depth beneath the root zone between 30 and 300 cm. In most soils except silt, under grass vegetation capillary rise of groundwater becomes very small for any water table depth larger than 300 cm. For that reason, application of model results is not restricted to soils ≤ 300 cm groundwater table depth. Since the effect of hill slopes was not taken into account, the surface storage was set to 2 cm to avoid surface runoff.

The model calculates potential evapotranspiration as grass reference evapotranspiration (Penman-Monteith method, Allen *et al*., 1989) for a minimal crop resistance. SWAP uses the Feddes function to reduce actual transpiration compared to grass reference evapotranspiration if it is delimitated by soil water content. The reduction coefficient for root water uptake is a function of the soil water pressure head and the potential transpiration rate. Since the proposal of Metselaar (2007) did not lead to reasonable results, the soil water pressure head below which uptake reduction starts was based upon the corresponding soil water content in terms of plant available water (Table 2). In the wet range of soil moisture, lack of aeration may lead to reducing plant water uptake. It was assumed that a minimum volumetric air content of 5 to 7% (Scheffer and Schachtschabel, 1998) would yield severe anaerobiosis. To define anaerobiosis by air content alone seems to be a very rough approximation. For that reason, clayey soils were simulated using two options. The first option includes a reduction of transpiration below a critical air content of 0.05 cm^3 cm^{-3} in the root zone and the second option excluded anaerobiosis by assuming a critical air content of only 0.01 cm^3 cm^{-3} . The only crop conside- red here was grass of 12 cm height covering the soil surface completely over the entire year. This study makes no attempt to consider various crop conditions.

In this study, three sites with different meteorological conditions were selected (Table 3). Simulation periods started on April 1st 1961 and ended on March 31st 1991

covering the entire period of 30 years. Please note that the precipitation data used here was corrected for systematic measurement errors (Richter, 1995). When in winter months with formation of snow cover air temperature rises above zero degrees, the SWAP model considers the melting of snow. The weather station Magdeburg showed the driest conditions. To extend results even more towards semi-arid conditions, the weather record of this station was modified. The original record contained seven years out of 30 with precipitation excess (P - E_p > 0). These data were replaced by data of the seven driest years from the same station. As will be shown later, the generation of semi-arid conditions exerts a strong impact on the results. The entire data set generated comprises 135 simulations runs of 30 years each.

Bagrov recognized that the mean actual evapotranspiration, E_a, strongly depends on mean annual precipitation, P, and derived consequently the differential equation:

$$\frac{dE_a}{dP} = 1 - \left(\frac{E_a}{E_p}\right)^b, \qquad (2)$$

where: E_p – potential evapotranspiration (cm), b – coefficient of efficiency according to Glugla *et al*. (2003).

In the case of arid conditions, when potential evapotranspiration E_p is large and actual evapotranspiration E_a is low, E_a/E_P is very small or approaches zero. It follows that dE_a/dP will approach 1 and the entire precipitation evaporates. Under conditions like these, actual evapotranspirations depends to a large extend on precipitation. From the opposite condition of excess precipitation follows that E_a/E_P will approach unity. Therefore, dE_a/dE_P becomes very small or almost zero. Since E_a then is approximately equal to E_p, the dependence of E_a on P vanishes. In the first case, water availability dominates evapotranspiration and in the second case energy availability is crucial. Thus, evapotranspiration is strongly limited either by water or by energy availability. Regarding these basic conditions (Eq. (2)) is a plausible simplification of the complex processes of real evapotranspiration. Based on Eq. (2) Glugla and Tiemer (1971), and Glugla *et al*. (2003) suggested estimating actual evapotranspiration from:

$$P = \int_0^{E_a} \frac{1}{1 - \left(E_a / E_p\right)^b} \, dE, \qquad (3)$$

where: E – variable of integration.

As the main advantage of Eq. (3) we would like to emphasize its property to restrict E_a either to precipitation, P, or to potential evapotranspiration, E_p. Intermediate values of E_a are governed by the so-called Bagrov coefficient b. This parameter represents the availability of soil water to evapotranspiration and depends on the amount of plant available soil water and capillary rise from groundwater. The Bagrov coefficient may vary between 0.5 for very restricted availability of soil water and about 8 for conditions of optimal evapotranspiration. The effect of b on actual evapotranspiration is shown in Fig. 1. This diagram could be used to evaluate Eq. (3) numerically. However, using the computer code provided is much more convenient.

T a b l e 3. Mean values of P and E_p at 3 locations (1961-1990)

Location	Average (cm)			
	annual		summer	
	P	E_p	P_s	$E_{p,s}$
Bremen	79.6	69.8	42.2	54.6
Uelzen	68.8	59.7	38.4	48.0
Magdeburg, modified	49.0	69.7	27.2	55.5

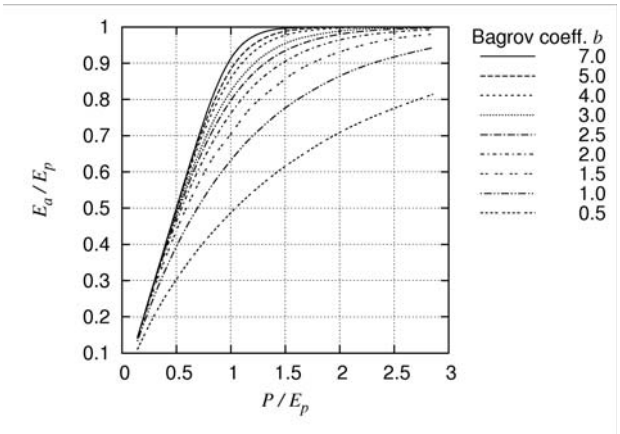

Fig. 1. Effect of the Bagrov coefficient, b, on actual evapotranspiration E_a.

There are two different conditions where the Bagrov method fails:

– because of the underlying assumption that infiltrated soil water be available to evapotranspiration, the method requires the residence time of infiltrated water in soil to be sufficient to make water available to evapotranspiration. This assumption is not met on sites with steep slope or with heavy storms on soils which exhibit at least temporarily an extremely high hydraulic conductivity,

– for plains under dry climatic conditions where the aquifer is recharged by groundwater inflow from regions with precipitation excess. Since Eq. (3) restricts actual evapotranspiration to precipitation, it should not be used for wetlands where E_a is enhanced by capillary rise from the groundwater table so much that it might exceed the local precipitation leading to groundwater depletion.

Both of these limitations require a different method to estimate actual evapotranspiration.

RESULTS

The unknown parameter b may be estimated by a transfer function from data which are in general easily available. The best agreement between SWAP-simulated and Bagrov-estimated actual evapotranspiration was obtained by a transfer function of the form:

$$b = c_1 W_a^{c2} + c_3 \exp(c_4\ q_{\max}) + c_5 \frac{C_s}{P_s - E_{p,s}}, \quad (4)$$

where: the variables $q_{\max}$ and C_s are explained below, P_s is precipitation, $E_{p,s}$ potential evapotranspiration during summer months (from April to September) and the coefficients $c_1 \cdots c_5$ are fitting parameters. W_a denotes the maximum plant available soil water storage given by:

$$W_a = d_r[\theta(-63) - \theta(-15850)], \quad (5)$$

where: d_r – rooting detph (cm), θ – soil water content as a function of soil water pressure head.

Parameters needed to evaluate Eq. (5) are shown in Tables 1 and 2. Please note that W_a represents a soil and crop property which does not depend on evapotranspiration. In the context of this investigation, both of the pressure head values selected to represent field capacity and permanent wilting point are arbitrary variables to express corresponding soil hydraulic properties in Eq. (4). The detailed discussion of field capacity is shown in Twarakavi (2009) and Zacharias and Bohne (2008) papers.

To consider the effect of capillary rise of water from the groundwater table to the root zone, an arbitrary steady-state flow rate, $q_{\max}$, is chosen which approximates the maximum flow rate to be expected under most conditions. The pressure head profile for any chosen $q_{\max}$ is given (Bohne, 2005; Jury *et al.*, 1991) as:

$$z(q_{\max}, h_{\min}) = \int_0^{h_{\min}} \left(\frac{q_{\max}}{K(h)} + 1\right)^{-1} dh, \quad (6)$$

where: z – vertical coordinate, z = 0 at groundwater table (cm), q – flow rate (cm day^{-1}), $K(h)$ – unsaturated soil hydraulic conductivity (cm day^{-1}), h – soil water pressure head (cm) and was calculated numerically. For $K(h)$, the van Genuchten-Mualem model of hydraulic conductivity was used (van Genuchten, 1980). A pressure value threshold of $h_{\min}$ = -3 200 hPa was chosen to obtain an approximate maximum capillary steady-state flow rate depending solely on soil hydraulic properties and flow distance, z. The advantage of this threshold is that data on unsaturated soil hydraulic conductivity to some extent are still available in this range (Renger *et al.*, 2009). Using Eq. (6) and soil hydraulic parameters as shown in Table 1, flow rates of texture classes were calculated. To bypass the processing of Eq. (6), an easy-to-use approximation was prepared, which is given by:

$$q_{\max}(z) = p_1 z^{p2}. \quad (7)$$

The parameters p_1 and p_2 depend on texture class and are shown in Table 4. Please note, that $q_{\max}$ describes steady-state maximum flow rates depending solely on soil hydraulic conductivity of the layer below the rooting zone and the flow distance z between the groundwater table and the lower boundary of the rooting zone without any regard to site, climate, and plant specific conditions.

T a b l e 4. Parameters of Eq. (7) holding for soil hydraulic parameters suggested by Renger *et al.* (2009)

Texture class	p_1	p_2	Texture class	p_1	p_2
Ss	$1.524\ 10^3$	-2.447	Uu	$9.690\ 10^3$	-2.100
Sl2	$1.834\ 10^3$	-2.383	Uls	$2.766\ 10^3$	-1.918
Sl3	$5.875\ 10^3$	-2.528	Us	$1.948\ 10^3$	-1.840
Sl4	$5.183\ 10^2$	-1.793	Ut2	$3.835\ 10^3$	-1.989
Slu	$5.657\ 10^2$	-1.721	Ut3	$3.712\ 10^3$	-1.986
St2	$3.971\ 10^2$	-1.497	Ut4	$3.078\ 10^3$	-2.008
St3	$2.265\ 10^2$	-1.804	Tt	$6.213\ 10^1$	-1.805
Su3	$8.504\ 10^2$	-1.742	Tl	$9.920\ 10^1$	-1.869
Su4	$1.299\ 10^3$	-1.736	Tu2	$9.814\ 10^1$	-1.864
Ls2	$1.486\ 10^3$	-1.586	Ts2	$2.229\ 10^2$	-1.963
Ls3	$9.739\ 10^2$	-1.794	Ts3	$8.573\ 10^2$	-2.103
Ls4	$7.201\ 10^2$	-1.766	Ts4	$2.070\ 10^2$	-1.520
Lt2	$7.615\ 10^2$	-1.762	fS	$3.020\ 10^3$	-2.481
Lt3	$3.886\ 10^2$	-1.671	mS	$1.566\ 10^3$	-2.454

Both of the influencing variables discussed so far describe the availability of soil water for evapotranspiration. Actual evapotranspiration further depends on the simultaneity of atmospheric evapotranspiration demand and atmospheric water supply (Glugla *et al.*, 2003). If seasons with high potential evapotranspiration happen to be without rainfall, actual evapotranspiration will be substantially lower than it would be in the case of evenly distributed rainfall. Based on thirty-year averages of monthly potential evapotranspiration and precipitation a coefficient of simultaneity was established which is given by:

$$Cs = \frac{\sum_{i=4}^{9} MAX(E_{p,i} - P_i);0}{\sum_{i=4}^{9} E_{p,i}}, \qquad (8)$$

where: P and E_p denote long-term averages of monthly sums of precipitation and potential evapotranspiration, respectively. The expression *MAX* stands for a function that returns the largest of the arguments given to it. The index i denotes the months from April to September.

To find the parameters of the transfer function Eq. (4) was substituted into Eq. (3) and the standard error of the predicted actual evapotranspitration was minimized by a FIBONACCI procedure (Vardavas, 1989). Integrations were performed by the Simpson procedure and the implicit calculation of E_a was done by the Newton algorithm. Because of the limitations of the Bagrov method as mentioned above, only two of the weather records were used to fit Eqs (3) and (4) to SWAP-generated data of actual evapotranspiration. The third record, which was modified to represent semi-arid conditions, yielded substantial groundwater depletion and thus, a disturbance of the local hydrological equilibrium. The results are shown in Table 5 and Fig. 2. Equation (3) predicts the actual evapotranspiration with a standard error of 1.55 cm.

The results discussed so far refer to soils without the influence of anaerobiosis. For groundwater-affected clay soils the Bagrov, b, parameter obtained from Eq. (4) should be modified according to:

$$b_a = b - c_6 (h_a - c_7) q_{\max}^{c_8} + c_9 \theta_{FC}, \qquad (9)$$

where: h_a denotes the soil water pressure head at the air content of 0.05 cm^3 cm^{-3}, $\theta_{FC} = \theta$ (-63 hPa) is field capacity and b_a is the Bagrov coefficient corrected for anaerobiosis. The fitting coefficients, c_i, are shown in Table 5. In the data base used are 15 data sets out of 135 showing anaerobiosis. The standard deviation between b_a and b is 1.144.

If the long-term average of actual evapotranspiration exceeds precipitation, the limitations of the Bagrov method mentioned above require application of a different method. Based on the entire data base comprising 3 long-term weather records, a statistic prediction equation was set up which is given by:

T a b l e 5. Values of the fitting parameters of Eqs (4), (9), and (10)

Parameter	Value	Parameter	Value
c_1	0.180	c_8	0.535
c_2	1.088	c_9	-11.832
c_3	1.791	c_{10}	0.054
c_4	2.588	c_{11}	0.017
c_5	52.421	c_{12}	0.701
c_6	0.058	c_{13}	0.903
c_7	0.274	c_{14}	0.010

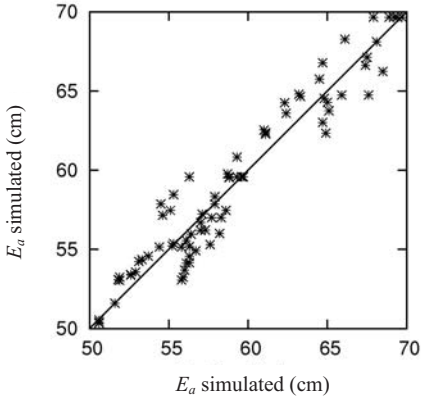

Fig. 2. Comparison between simulated and estimated actual evapotranspiration, E_a.

$$\frac{E_a}{E_p} = c_{10} + c_{11} P_s + c_{12} q_{\max}^{c_{13}} + c_{14} W_a. \qquad (10)$$

Equation (10) predicts the relation E_a/E_p using the long-term average of summer precipitation, P_s (from April to September). The remaining variables keep their meaning as explained above. It has been shown that during winter the difference between potential and actual evapotranspiration is negligible (Wessolek *et al.*, 2011). Hence, from Eq. (1) groundwater recharge, R, is obtained by:

$$R = P - E_p + E_{p,s}\left(1 - \frac{E_a}{E_p}\right), \qquad (11)$$

where: $E_{p,s}$ – denotes the potential evapotranspiration during summer (from April to September).

The parameters of Eq. (11) are shown in Table 5. Equation (11) predicts groundwater recharge with an standard error of RMSE = 2.581 cm. Please note that this value was obtained from the fitting procedure, not from applying the method to an independent data set. The coefficient of correlation between SWAP-simulated and predicted groundwater recharge is R = 0.975. Figure 3 displays results

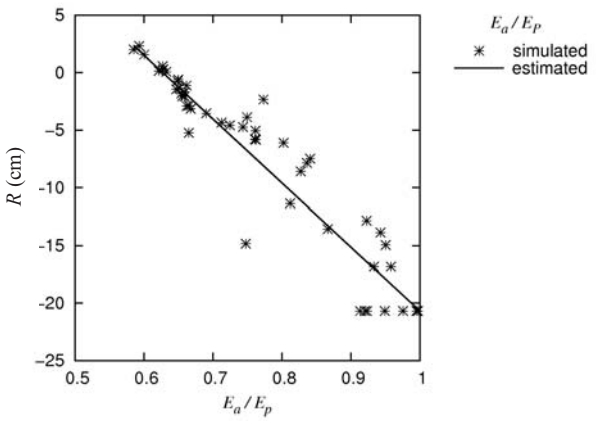

Fig. 3. Groundwater recharge, *R*, *vs*. simulated and estimated relation E_a/E_p under arid climatic conditions.

obtained from Eq. (11) *vs*. groundwater recharge. For $E_a/E_p > 0.6$ groundwater gets depleted. Because of high potential evapotranspiration, capillary water supply from groundwater is forced to meet the atmospheric demand.

CONCLUSIONS

1. The study has shown that it is feasible to estimate regional long-term groundwater recharge from easily available data. These are precipitation, potential evapotranspiration, soil texture and depth to groundwater.

2. There are two ways to estimate actual evapotranspiration and groundwater recharge. If precipitation is higher than evapotranspiration, using the Bagrov method is suggested. This method is expected to yield reliable results under different conditions and its errors are tolerable. The method contains only one unknown parameter, which can be estimated by a transfer function. Since the Bagrov method restricts actual evapotranspiration to precipitation, it cannot be used for parts of catchments where long-term actual evapotranspiration is in excess over precipitation. In this study, a purely statistic based method is provided to cover the general case.

3. The method described is meant for application in lowlands and its results need to be scrutinized.

4. It is expected that the method yields a reasonable first guess which may be improved by regional calibration.

REFERENCES

Allen R.G., Wright M.E., and Burman R.D., 1989. Operational estimates of evapotranspiration. Agron. J., 81, 650-662.

Bohne K., 2005. An Introduction into Applied Soil Hydrology. Catena Verlag Reiskirchen, Germany.

Bonta J. and Müller M., 1999. Evaluation of the Glugla method for estimating evapotranspiration and groundwater recharge. Hydrol. Sci., 44(5), 743-761.

Glugla G., Jankiewicz P., Rachinow C., Lojek K., and Richter K., 2003. BAGLUVA - Wasserhaushaltsverfahren zur Berechnung vieljähriger Mittelwerte der tatsächlichen Verdunstung und des Gesamtabflusses. Bundesanstalt für Gewässerkunde, Koblenz, Germany.

Glugla G. and Tiemer K., 1971. Ein verbessertes Verfahren zur Berechnung der Grundwasserneubildung. Wasserwirtschaft, Wassertechnik, 20(10), 349-353.

Jury W.A., Gardner W.R., Gardner W.H., 1991. Soil Physics. Wiley Press, New York, USA.

Kroes J.G. and van Dam J.C. (Eds), **2003.** Reference Manual SWAP version 3.0.3. Alterra Report, 773, Wageningen, the Netherlands.

Kroes J.G., van Dam J.C., Huygen J., and Vervoort R.W., 1999. Simulation of water flow, solute transport and plant growth in the Soil-Water-Atmosphere-Plant environment: User's Guide od SWAP version 2. Technical Document Nr. 53 DLO Winand Staring Centre, Wageningen, the Netherlands.

Luckner L., van Genuchten M.T., and Nielsen D.R., 1989. A consistent set of parametric models for the two-phase flow of immiscible fluids in the subsurface. Water Resour. Res., 25, 10, 2187-2193.

Metselaar K. and de Jong van Lier Q., 2007. The shape of the transpiration reduction function under plant water stress. Vadose Zone J., 6, 124-139.

Renger M., Bohne K., Facklam M., Harrach T., Riek W., Schäfer W., Wessolek G., and Zacharias S., 2009. Bodenphysikalische Kennwerte und Berechnungsverfahren für die Praxis. Bodenökologie Bodengenese, 40, 20-26.

Richter D.U., 1995. Ergebnisse methodischer Untersuchungen zur Korrektur des systematischen Messfehlers des Hellmann-Niederschlagsmessers. Berichte des Deutschen Wetterdienstes, 194, Offenbach, Germany.

Scheffer F. and Schachtschabel P., 1998. Lehrbuch der Bodenkunde. Ferdinand Enke Verlag, Stuttgart, Germany.

Twarakavi N., 2009. An objective analysis of the dynamic nature of field capacity. WRR45, W10410 doi: 10.1029/2009WR007944.

Twarakavi N., Simunek J., and Schaap G., 2010. Can texture-based classification optimally classify soils with respect to soil hydraulics? Water Resour. Res., 46, W01501, doi:10.1029/2009WR007939.

van Dam J.C., Groenendijk K.P., Hendriks R.F.A., and Kroes J.G., 2008. Advances of modeling water flow in variably saturated soils with SWAP. Vadose Zone J., 7(2), 640-653.

van Genuchten M.T., 1980. A closed-form equation for predicting the hydraulic conductivity of unsaturated soils. Soil Sci. Soc. Am. J., 44, 892-898.

Vardavas I.M., 1989. A Fibonacci search technique for model parameter selection. Ecol. Modeling, 48, 65-81.

Wessolek G., Bohne K., Duijnisveld W., and Trinks S., 2011. Development of hydro-pedotransfer functions to predict capillary rise and actual evapotranspiration for grassland sites. J. Hydrol., 400, 429-437.

Wessolek G., Duijnisveld W.H.M., and Trinks S., 2008. Hydropedotransfer functions (HPTFs) for predicting annual percolation rate on a regional scale. J. Hydrol., 356, 17-27.

Zacharias S. and Bohne K., 2008. Attempt of a flux-based evaluation of field capacity. J. Plant Nutr. Soil Sci., 171(3), 399-408.